SARS-CoV-2 Fusion Peptide-Directed Antibodies Elicited by Natural Infection Mediate Broad Sarbecovirus Neutralization

Alex L. Roederer[1], Yi Cao[1], Chia Jung Li[1], Eunice Lim[1], David H. Canaday[2,3], Stefan Gravenstein[4,5,6], Alejandro B. Balazs[1,*]

[1]Ragon Institute of MGH, MIT, and Harvard, Cambridge, MA, 02139, USA

[2]Case Western Reserve University School of Medicine, Cleveland, OH

[3]Geriatric Research Education and Clinical Center, Louis Stokes Cleveland Department of Veterans Affairs Medical Center, Cleveland, Ohio

[4]Center of Innovation in Long-Term Services and Supports, Veterans Administration Medical Center, Providence, Rhode Island

[5]Division of Geriatrics and Palliative Medicine, Alpert Medical School of Brown University, Providence, Rhode Island, USA.

[6]Brown University School of Public Health Center for Gerontology and Healthcare Research, Providence, Rhode Island

[7]University of California, San Francisco, California

*Lead Contact, correspondence: abalazs@mgh.harvard.edu

SUMMARY

Studies have demonstrated that repeated mRNA vaccination enhances the breadth of neutralization against diverse SARS-CoV-2 variants. However, the development of antibodies capable of neutralizing across the Coronavirinae subfamily is poorly understood. In this study, we analyze serum samples to determine their neutralization breadth and potency and identify their antigenic targets. Using a cohort of older individuals and healthcare workers, we track correlates of broad neutralizing responses, including fusion peptide (FP) antibody elicitation. We find that although broadly neutralizing responses are often a result of RBD-specific antibodies, a rare subset of donors produce FP-specific broadly neutralizing responses. Interestingly, FP-specific antibodies are not observed in COVID-naive individuals irrespective of vaccination regimen, but rather, they occur following natural infection or vaccine breakthrough. This study highlights the epitope targets underpinning broadly neutralizing antibody responses to coronaviruses and suggests that existing vaccines are insufficient to promote the elicitation of FP-directed broadly neutralizing coronavirus antibodies.

KEYWORDS: COVID-19; SARS-COV-2; broad neutralization; fusion peptide; stem helix; neutralizing antibodies

Introduction

SARS-CoV-2 first appeared at the end of 2019 in Wuhan, China and quickly spread across the world, infecting more than 700 million people and causing 7 million deaths[1]. The global impact of this virus resulted in the development of multiple monoclonal neutralizing antibodies and vaccines to limit disease severity. The spike protein is the predominant site of neutralizing antibodies against SARS-CoV-2. The spike is composed of two subunits, the S1 which contains the receptor binding domain (RBD) and the N-Terminal Domain (NTD), and the S2, which contains the highly conserved Fusion Peptide (FP), Stem Helix (SH) and fusion machinery. The RBD is the predominant target of neutralizing antibodies given its role in binding to the ACE2 receptor on host cells[2]. In the first year of the pandemic, numerous monoclonal antibodies targeting the RBD were approved for treatment but have since been rendered ineffective due to escape by SARS-CoV-2 variants[3–5]. This escape highlights the urgent need for preventive therapies including vaccines that will more effectively target future variants.

COVID-19 vaccination has been critical for prevention of significant disease from SARS-CoV-2 worldwide. The first generation of COVID vaccines[6–9] were based on the Wuhan strain of SARS-CoV-2 spike protein, containing 2 proline-stabilizing mutations that were previously used to stabilize other related spike proteins[10]. SARS-CoV-2 variants have arisen over the last four years that have contributed to immune evasion and changes in viral infectivity[11–17]. The vaccine has been reformulated three times, first to a bivalent composition of Wuhan and BA.5 variant spike sequences[18–21], and then to a monovalent XBB.1.5 spike sequence[22–25], and recently to a monovalent KP.2 spike sequence[26].

Despite these reformulations being highly effective against the variants they are composed of, the virus continues to mutate with the JN.1 and KP.2 variants escaping XBB.1.5 boosted sera effectively[17,27,28]. JN.1 and offshoot variants including KP.2 currently make up over 96% of all sequences being submitted to the GISAID database[29]. A majority of mutations in variants have occurred in the RBD region with JN.1 and KP.2 having 28-29 of their 58-61 mutations in the RBD, driving the escape of the humoral immune response[27–31].

Despite the plethora of vaccines, the virus has continued to evade humoral immune responses due to the immunodominance of RBD-directed antibodies and the selective pressure on this region. Notably, the FDA met in the summer of 2024 to formulate a vaccine for 2025[32], suggesting that COVID vaccines will continue to be updated annually, much like those for Influenza, potentially costing billions each year[33,34]. Understanding the nature of rare broadly neutralizing responses to SARS-CoV-2 in patients is crucial for the development of next-generation vaccines that can uniformly elicit broadly neutralizing coronavirus antibodies.

Ideally, coronavirus broadly neutralizing antibodies would neutralize all existing SARS-CoV-2 variants and provide cross-reactivity to pre-endemic strains likely to emerge in the future. Therefore, future vaccines could target highly conserved regions within the spike protein. There are several highly conserved regions within the RBD among SARS-CoV-2 variants that can be targeted by neutralizing antibodies[35,36]. However, it has been theorized that the mutational landscape in the RBD is incredibly vast[37], and strong immune pressure has consistently selected for the RBD escape mutations found in existing variants. The SH is conserved among betacoronaviruses while the FP is conserved among all coronaviruses. Multiple groups have identified broadly cross-reactive and neutralizing antibodies that target these less common epitopes[38–45]. Given its conservation across even distantly related coronaviruses, the FP represents an ideal target antigen for vaccine design, however it is unclear how these neutralizing antibodies to FP are elicited.

To understand the development of broadly neutralizing antibody responses, we characterized donor sera with widely different neutralizing potency and breadth for binding to conserved antigenic sites within the spike protein. Interestingly, we find that the most potent neutralizers have the highest RBD, SH and FP titers despite similar spike titers as less potent donors. Furthermore, among broad neutralizers we find that RBD and FP specific antibodies correlate with neutralizing titer to SARS-CoV-2. To further understand the make-up of a broadly neutralizing antibody response, we selectively depleted antibodies to the RBD, FP and SH. We find that while RBD antibodies are predominantly responsible for broad neutralization, as others have seen[40,46–48], there exist rare donors with neutralizing FP antibodies that contribute significantly to breadth, however, FP antibody development is limited in most donors. Importantly, we find that FP antibodies develop following natural infection, and that additional vaccination leads to a decline in FP-specific antibody titers. Taken together, these results highlight the shortcomings of existing vaccination regimens to elicit highly cross-reactive, broadly neutralizing antibodies.

RESULTS

Broad neutralizers have extensive breadth across related Betacoronaviruses.

To investigate the breadth of neutralization, a cohort of 399 donors were evaluated for WT, BA.1 or BA.5 spike pseudovirus neutralization (**Figure S1A**). Notably, some donors exhibited potent neutralizing activity against all three viruses, exceeding the limit of detection of our assay. Donors were binned into distinct groups based on average neutralizing titer across the three variants (**Figure 1A**). Donors were classified as *broad-potent*, *narrow-potent*, *moderate*, and *weak* neutralizers. To determine whether these broadly neutralizing responses could extend to other human infecting coronaviruses we developed high throughput neutralization assays for pseudoviruses representing these diverse viruses. Given that 229E and MERS use human Aminopeptidase (hANPEP)[49,50] and dipeptidyl peptidase-4 (hDPP4)[51,52] as cell receptors, stable cell lines expressing these cell-surface proteins were developed and confirmed to express their respective receptors by flow cytometry (**Figure S1B, C**). Each cell line was susceptible to their respective pseudoviruses and neutralization assays with previously described neutralizing antibodies resulted in IC_{50} values that were similar to those previously reported[44,53] (**Figure S1D**).

A subset from each group of neutralizers were further tested against multiple related betacoronaviruses and two common cold alphacoronaviruses with a higher limit of detection to allow for more accurate assessment of maximum neutralizing titers (**Figure 1B**). The most potent and broad neutralizers exhibited activity against variants and SARS-like viruses, but this activity did not extend to other coronaviruses including NL63, 229E and MERS. *Broad-potent* neutralizers were further subdivided into *extra-potent* and *broad-potent* based on an average of pNT50 values against all betacoronaviruses except MERS, with *extra-potent* having a significantly higher average NT_{50} of 6971 while *broad-potent* had an average of 1455 (**Figure 1C**). While *broad-potent* sera exhibited extensive activity against SARS-CoV-2 WT, BA.1 and BA.5 variants, it lacked substantial neutralizing titer against related Betacornaviruses SARS-CoV-1 and WIV1 as compared to *extra-potent* sera.

Broad neutralizers harbor the highest levels of stem helix and fusion peptide antibodies.

Coronaviruses are highly diverse and split into four genera, alphacoronaviruses, betacoronaviruses, deltacoronaviruses and gammacoronaviruses. All coronaviruses enter cells using their spike proteins, but the species tropism and cell receptor usage varies. Aligning the spike sequences across all four genera by conservation[54] highlights that the RBD, the region for most neutralizing antibodies, are not conserved across coronaviruses (**Figure 2A**). The most conserved regions include the SH and the FP. The five groups of neutralizing donors were

assessed for their ability to bind to the spike, RBD, SH, and FP by Enzyme Linked Immunosorbent Assays (ELISA). Anti-spike (**Figure 2B**) and anti-RBD (**Figure 2C**) antibody endpoint titers were significantly higher for the *extra potent*, *broad potent*, and *narrow potent* groups than the *moderate* or *weak* neutralizers, as expected. Notably, the *extra potent* group had slightly lower levels of spike-binding antibodies but higher levels of RBD-directed antibodies than the *broad potent* group. Surprisingly, *extra potent* neutralizers were the only group to have significantly higher anti-SH (**Figure 2D**) and anti-FP (**Figure 2E**) antibodies than *weak* and *moderate*, suggesting that the increased potency of these samples may be due to antibodies targeting these epitopes.

We calculated the relative neutralization potency of each humoral immune response targeting Spike or RBD by normalizing pNT50 values by the endpoint titer for each serum sample. Interestingly, only *extra potent* neutralizers had significantly higher potency than *broad potent* neutralizers (**Figure S2A**) indicating that despite the *broad potent* group producing large amounts of antibody, many of those are non-neutralizing. *Extra potent* donors also exhibited significantly higher neutralizing potency when normalizing for antibodies targeting RBD, suggesting that targeting this epitope leads to a greater proportion of antibodies capable of neutralizing virus (**Figure S2B**).

RBD and fusion peptide specific antibodies correlate with neutralizing titer.

To investigate the effect of antigen specific antibodies on neutralizing titer we selected 8 *extra potent* donors who had multiple serum collections over time (**Table S1**). Donors were older individuals with an average age of 71. All donor timepoints were assessed for their antibody titers against spike, RBD, SH and FP (**Figure 3A**) to determine the amounts of antibody targeting each epitope. Known antibodies specific for each epitope were used to establish standard curves to interpolate Unit/mL values for each sample. A non-specific control antibody at the same serum IgG concentration was used to determine a cutoff for background binding to the FP and SH (**Figure 3B**). 11/19 serum timepoints (from 4 donors) reached the FP cutoff threshold and 9/19 serum timepoints (from 4 donors) reached the SH cutoff threshold (**Figure 3B**). Of note, one donor had neither FP nor SH activity despite being *extra potent*, which could be due to very broad and potent RBD-directed antibodies. To assess whether antigen-specific antibodies had an impact on SARS-CoV-2 neutralizing titer, correlation matrices were created for anti-spike (**Figure 3C**), anti-RBD (**Figure 3D**), anti-SH (**Figure 3E**) and anti-FP (**Figure 3F**) binding measurements. SH and FP correlation matrices only contained samples falling above their respective background levels. Despite the limited sample size, RBD and FP binding titers both correlated with the WT SARS-

CoV-2 spike neutralizing titer, while spike and SH binding titers did not correlate with neutralization.

Given the correlations with neutralizing titer, we sought to understand the effect of vaccination on the development of antigen specific antibodies with our cohort. Generally, each vaccine dose increased SARS-CoV-2 spike and RBD specific antibodies, while antibody responses went down over time between doses (**Figure S3A**). Despite this, samples taken from individuals who had received all vaccines and boosters exhibited high levels of RBD and Spike antibodies. There was no trend observed for FP or SH specific antibodies. Unsurprisingly, SARS-CoV-2 vaccination showed no impact on the neutralizing titers of the alphacoronaviruses NL63 (**Figure S3B**) or 229E (**Figure S3C**), and no donor was able to neutralize MERS, irrespective of vaccination (**Figure S3D**). This suggests that while breadth extends to SARS-CoV-2 variants and closely related viruses, it does not extend to distantly related coronaviruses.

Fusion peptide antibodies contribute to neutralization breadth.

To investigate the contributions to breadth of RBD, SH, and FP-specific antibodies, we selectively depleted SARS-CoV-2 domain or peptide-specific antibodies using magnetic beads (**Figure 4A**). Mock depletions are performed by mixing the beads with serum without antigen. Depletions were highly selective against the depleting antigen for both his-tagged WT SARS-CoV-2 RBD (**Figure S4A**), and maleimide coupled FP and SH (**Figure S4B**)**.** Using a subset of donor sera with the highest neutralizing activity, 8 donors with potent FP binding and 6 donors with potent SH binding (**Figure S4C, D**) were depleted for the respective antigen. Depletion of FP and SH-specific antibodies had a minimal effect on the neutralizing titers of donor samples against both SARS-CoV-2 (**Figure S4E**) and SARS-CoV (**Figure S4F**). Despite no general trend, a few donor timepoints (FP3, FP6) had slightly reduced neutralizing activity against both SARS-CoV and SARS-CoV-2 when depleted for FP-specific antibody binding while a single donor had slightly reduced neutralizing activity against both viruses after SH Depletion (SH4).

It has been previously shown that SARS-CoV-2 RBD depletion of sera can remove the majority of neutralizing activity[46–48,55,56]. To determine whether this would also be the case with potent neutralizing sera, we depleted 17 potently neutralizing samples using SARS-CoV-2 RBD (**Figure S4G**). Of note, donors 3,9,10,12,14,15, and 17 retained some neutralizing activity against SARS-CoV-2 (**Figure 4B**) after SARS-CoV-2 RBD depletion, while donors 3 and 17 retained substantial neutralizing activity against SARS-CoV after SARS-CoV-2 RBD depletion (**Figure 4C**). These results suggest that these donors harbor non-RBD, cross-reactive, neutralizing antibodies. As both donor 3 and 17 samples exhibited potent FP binding, the SARS-CoV-2 RBD-

depleted samples were further depleted to remove FP-binding antibodies (**Figure S4H**). While donor 17 retained some neutralizing activity to SARS-CoV-2 (**Figure 4D**), both donors lost all neutralizing activity against SARS-CoV (**Figure 4E**), suggesting that FP-specific responses in these donors were responsible for significant neutralizing activity. Taken together, we find that some donors harbor FP-specific neutralizing antibodies that can contribute to neutralizing activity, particularly against other coronaviruses.

Fusion peptide specific antibodies arise only from natural infection

Given the variability of FP-specific antibody levels we measured across donors, we sought to determine when FP-specific antibodies arose. Using a cohort of pre-vaccine COVID+ donor serum samples (**Table S2**), we found that more severe COVID infections led to higher FP-specific antibody levels. (**Figure 5A**). We found no differences in FP titers regardless of age (**Figure S5A**), race (**Figure S5B**) or biological sex (**Figure S5C**).

We next sought to determine the effect of vaccinations on FP-specific antibody elicitation. Donor samples were gathered from aged-matched cohorts containing older individuals to test for FP-specific responses by ELISA (**Table S2**). COVID-naive and COVID-experienced donors were first compared to determine whether FP-specific antibodies are present in sera obtained before SARS-CoV-2 vaccines were available (**Figure 5B**). As expected, donors who were COVID-experienced had significantly higher levels of FP-specific antibodies than naive donors, signifying that FP antibodies are not present prior to infection or vaccination. To assess the effects on FP-specific antibody development once vaccines became widely distributed, samples from COVID-naive donors or COVID-experienced donors obtained post-vaccination were compared by FP antibody ELISA. COVID-experienced donors had significantly higher levels of FP-specific antibodies (**Figure 5C**). Simultaneously, a longitudinal cohort consisting of samples taken from COVID-naive donors from pre-vaccination to XBB.1.5 booster (**Table S2**) was tested for FP-specific antibodies. Interestingly, all donors had background levels of FP-specific antibodies irrespective of vaccination or boosting (**Figure 5D**). However, longitudinal timepoints obtained for COVID-naive donors who experienced breakthrough infection between their WT booster and bivalent vaccines, showed a significant increase in FP-specific antibodies between the pre-breakthrough timepoint and the breakthrough time point (**Figure 5E**). There was an apparent decrease in FP-specific antibodies after bivalent vaccines and XBB.1.5 booster, though these differences did not reach statistical significance. These data suggest that existing vaccine designs do not stimulate the development of FP-specific antibodies and may instead decrease FP-specific responses that arise with breakthrough infection.

Discussion

We sought to uncover how broad neutralization of SARS-CoV-2 and related coronaviruses developed following vaccination or infection and assessed the contribution of various spike epitopes to broad recognition. To this end, we determined the neutralization potency of hundreds of donors to find those with the most potent and broad neutralization. We found that neutralization activity in sera from *extra potent* neutralizers predominantly arises from RBD-specific antibodies as has been previously reported[57]. However, *extra potent* neutralizers also had the highest levels of SH and FP-specific antibodies. Moreover, among the *extra potent* neutralizing timepoints, only RBD and FP-specific antibodies correlated with neutralizing titer. Despite increases in spike and RBD antibodies we observed over multiple vaccine administrations, there was no correlation between vaccination and the development of SH and FP-specific responses. In line with this, neutralization breadth driven by vaccination extended to SARS-CoV-2 variants and SARS-like viruses, but did not extend to more distantly related beta and alpha coronaviruses.

Depletion of SARS-CoV-2 RBD-specific antibodies drastically reduced neutralization potency of sera, while FP-specific depletion resulted in only minimal effects, suggesting that the vast majority of neutralization can be attributed to RBD-specific humoral immunity. However, rare donors maintained substantial neutralizing titers against SARS-CoV-2 and SARS-CoV after RBD-specific depletion, indicating the presence of cross-reactive neutralizing antibodies targeting an epitope outside of RBD. Serial depletion of RBD followed by FP resulted in loss of all neutralizing activity, confirming the potential for FP-specific antibodies to contribute to neutralization activity. Our results agree with previously published work showing that depletion of convalescent donor serum with a linear peptide including the FP reduced neutralization titers by only 20%[58]. Additionally, our results suggest the activity of RBD-specific antibodies can mask FP-directed neutralizing antibodies, and that RBD depletion is necessary to enable their detection. This is especially true given the wide range of neutralization potencies of monoclonal FP-specific antibodies against SARS-CoV-2[42–45].

Given their potential use as broad-spectrum treatments against coronaviruses, we sought to determine the source of FP-specific antibody development. Comparing COVID-naive to COVID-experienced cohorts, we found a clear, significant increase in FP-specific antibodies in COVID-experienced donors suggesting that FP-specific antibodies develop in response to natural infection. It is known that FP-specific antibodies lack binding to recombinantly expressed spikes, which contain either 2 or 6 proline mutations to stabilize the trimer[45]. mRNA vaccines all encode spike proteins with the 2 proline mutations, which may explain their lack of elicitation of FP-specific antibodies in vaccinated, COVID-naive individuals. Indeed, we found that no amount of mRNA

vaccinations promoted FP-specific antibody development, while vaccination after infection in a breakthrough cohort largely decreased FP-specific responses. While age, gender, and demographics were not correlated with FP-specific antibody development, COVID severity tended to induce higher levels of FP-specific antibodies. This may be due to the extremely high levels of spike-specific antibodies seen in severe COVID cases as we and others have shown a correlation between the amount of spike-specific antibodies and disease severity[59,60,60].

Our study predominantly utilized samples from a cohort of nursing home donors who have been longitudinally profiled, highlighting a unique cohort which generally struggles to maintain effective immunity against continued SARS-CoV-2 evolution. However, we were able to find donors among these with very broad and potent neutralizing activity, demonstrating the potential to create effective humoral responses. These results also highlight the deficiencies of current vaccines for the generation of broadly neutralizing coronavirus antibodies, suggesting that updated vaccination approaches are needed. Updated domain-specific vaccines have demonstrated promising results in clinical trials[61], however, these lack FP sequences. In contrast, S2-specific vaccines also have shown potential for protection and contain the FP-region which may improve targeting of this epitope[62,63]. FP-specific vaccines have been suggested for HIV as a means of specifically eliciting antibodies against this target[64,65]. Whether similar vaccine designs presenting coronavirus FP could elicit comparable humoral responses remains to be determined.

Although the COVID-19 pandemic has been declared over by the WHO[66,67], there are still tens of thousands of cases and hundreds of deaths each day and the virus continues to evolve to evade humoral immunity[68]. Additionally, the ever-present threat of a new zoonotic transmission event, given the vast reservoir of SARS-like viruses that exist in animal populations, highlights the need to develop more broadly effective vaccines. Development of approaches capable of efficiently eliciting FP-specific antibodies would ensure the availability of effective prophylaxis against future pandemic coronaviruses.

Limitations of the Study

This study is limited to the evaluation of serum neutralizing antibodies to the spike protein using a pseudovirus-based neutralization assay, and does not take into account neutralizing antibodies to other proteins including the N and M proteins which may contribute to neutralizing breadth. Additionally, spike ELISAs used 2P-stabilized recombinant proteins, which could underestimate the total spike antibodies. It is known that FP-specific antibodies bind 2P-stabilized spikes with lower affinity than the native conformation of spike[45]. Our experiments also utilized

linear peptides to represent the FP and SH and therefore could be underestimating the binding to these epitopes in the context of the native conformation of spike, however, others[38,42–44] have used similar approaches for monoclonal antibody binding and for sorting of individual memory B cells.

RESOURCE AVAILABILITY

Lead Contact

Further information and requests for resources and reagents should be directed to and will be fulfilled by Alejandro Balazs (abalazs@mgh.harvard.edu).

Materials Availability

Plasmids generated in this study will be available through Addgene. Recombinant proteins, peptides, and antibodies are available from their respective sources.

Data and Code Availability

This study did not generate sequence data. Data generated in the current study (including neutralization measurements and flow cytometric files) have not been deposited in a public repository but are available from the corresponding author upon request. The code used to make the phylogenetic trees can be made available from the corresponding author upon request.

ACKNOWLEDGEMENTS, FUNDING SUPPORT

We wish to thank Michael Farzan, PhD, for providing ACE2-expressing 293T cells. This work was supported by the Peter and Ann Lambertus Family Foundation. A.B.B. was supported by NIAID R01s AI174875, AI174276, AI129709-03S1 the NIDA Avenir New Innovator Award DP2DA040254, the NIDA Avant-Garde Award 1DP1DA060607, a Massachusetts Consortium on Pathogenesis Readiness (MassCPR) grant, CDC subcontract 200-2016-91773-T.O.2 and a grant from Coalition for Epidemic Preparedness Innovations (CEPI).

AUTHOR CONTRIBUTIONS

Conceptualization: A.R., A.B.B.

Methodology: A.R., Y.C.

Samples: D.H.C., S.G., M.P

Investigation: A.R., Y.C., C.J.L, E.L, T.D.

Data Curation: A.R.

Writing – Original Draft: A.R.

Writing – Reviewing and Editing: A.R., A.B.B. edited the paper with input from co-authors.

DECLARATION OF INTERESTS

A.B.B. is a founder of Cure Systems LLC. S. G. and D. H. C. are recipients of investigator-initiated

grants to their universities from Pfizer to study pneumococcal vaccines, Sanofi Pasteur and Seqirus to study influenza vaccines, Moderna to study respiratory infection, and GSK to study herpes zoster. S. G. is the recipient of an investigator-initiated grant to the university from Genentech on influenza antivirals; reports consulting for GSK, Janssen/Johnson&Johnson, Merck, Novavax, Moderna, Seqirus, Sanofi, and Vaxart; he has received honoraria for speaking for AstraZeneca, Pfizer, Seqirus, Sanofi; reports personal fees from Pfizer; and reports data and safety monitoring board fees from Longevoron and SciClone.

Disclaimer. The contents do not represent the views of the U.S. Department of Veterans Affairs or of the United States Government.

MAIN FIGURE TITLES AND LEGENDS

Figure 1: Broad neutralizers have extensive breadth across related Betacoronaviruses.

(A) Cohort of 399 donor samples divided into 4 groups by average neutralization potency (average of n=2 technical replicates) across SARS-CoV-2 WT and the BA.1 and BA.5 variants. Groups were compared using a One-Way ANOVA with Holm-Šídák correction for multiple comparisons using statistical hypothesis testing **** = P<0.0001.

(B) 14 of the broadest neutralizers were subject to our high throughput neutralization assay against SARS-CoV-2, variants, SARS-like viruses, and other distantly related coronaviruses with a much higher threshold for neutralizing activity (average of n=2 technical replicates) . These donors were further subdivided into Super Potent and Broad Potent based on average neutralizing activity.

(C) Neutralizing activity (average of n=2 technical replicates) of donors averaged across Beta Coronaviruses (excluding MERS). Groups were compared using a two tailed Mann-Whitney T test with P = 0.0007.

Figure 2: Extra potent sera have the highest levels of RBD, SH and FP Antibodies.

(A) Conservation of the amino acids within the spike protein generated using consurf50 from (PDB 6XR859 https://doi.org/10.2210/pdb6xr8/pdb). The sequences fed into the algorithm include 59 coronavirus spike sequences representing all four clades. RBD = Receptor Binding Domain, NTD = N-Terminal Domain, FP = Fusion Peptide, SH = Stem Helix.

(B-E) Results from ELISA assessing the antibody endpoint titers of plasma from 22 extra potent, 13 Broad/Potent, 13 Narrow/Potent, 16 Moderate and 14 Weak donors. Antibody endpoint titers (average of n=2 technical replicates) were assessed against an S2P Stabilized spike (B), Receptor Binding Domain (C), Stem Helix Peptide (D), or Fusion Peptide (E). Antibody endpoint titer represents the maximum interpolated dilution that can still bind the antigen. The endpoint titers were evaluated at a top dilution of 100-fold with seven additional 3-fold serial dilutions. The wells incubated with no plasma incubation were used as controls, and cut-off values (used for interpolation) were defined as 2.1X the OD450 of the controls. Representative data from two independent experiments is shown. Groups were compared using a One Way ANOVA with Kruskal Wallis Test and Dunn's multiple comparisons test. (* = P<0.0332, ** = P<0.0021, ***= P<0.0002, ****= P<0.0001).

Figure 3: RBD and fusion peptide specific antibody titers correlate with neutralizing activity.

(A) U/mL of antigen specific antibody was assessed for a cohort of broad and potent neutralizers (average of n=2 technical replicates). All U/mL were calculated using an antigen specific ELISA and were defined as the equivalent reactivity to 1 μg/mL binding of the following antibodies: RBD182 (Spike, RBD), 76E1 (FP), S2P6 (SH).

(B) All donors from A were tested for binding to the Stem Helix or Fusion Peptide along with a negative control antibody (2A10) at the same concentration as the serum dilution to determine cutoffs to define background serum binding.

(C-F) Log-log regression analyses were performed on neutralization versus anti-Spike IgG (C), anti-RBD IgG (D), anti-SH IgG (E), and anti-FP IgG (F). Pearson correlations were performed and R^2 and p values are indicated.

Figure 4: Fusion peptide antibodies contribute to neutralization breadth.

(A) Schematic detailing our antigen depletion protocol. Briefly, his-tag or maleimide binding magnetic beads are pre-coupled to the antigen/peptide and mixed with serum. After an incubation the magnetic beads are pulled away using a magnet and serum is collected for downstream assays. Mock depletion is done by mixing serum and beads with no antigen (Created in BioRender).

(B-C) Serum samples with high neutralizing activity were subject to RBD based depletion using his-tagged beads or mock depletion using beads with no RBD bound. Mock and depleted serum was tested for neutralizing activity (average of n=2 technical replicates) against SARS-CoV-2 (C) and SARS-CoV (D).

(D-E) Serum samples with remaining neutralizing activity against both SARS-CoV-2 and SARS-CoV from (B-C) were subject to further depletion with the fusion peptide and tested for remaining neutralizing activity (average of n=2 technical replicates) to SARS-CoV-2 (D) and SARS-CoV (E) after double depletion.

Figure 5: Fusion peptide antibodies develop in response to natural infection.

(A) Anti-Fusion Peptide ELISA for a cohort of COVID+ pre-vaccination timepoints split into non-hospitalized and severity of hospitalization (average of n=2 technical replicates). Limit of detection line is defined as the background binding of a negative control antibody to the FP for that experiment. A Kruskal Wallis one-way ANOVA was performed with Dunn's correction for multiple comparisons.

(B) Anti-Fusion Peptide ELISA (average of n=2 technical replicates) for pre-vaccination serum samples for donors who were naïve or who had been infected with COVID. A Mann Whitney Two tailed T-test was performed to assess significance.

(C) Anti-Fusion Peptide ELISA (average of n=2 technical replicates) for post-vaccination serum samples for donors who were naïve after 2-6 vaccines or who were COVID+ at the timepoint and had received between 2-6 vaccines. A Mann Whitney Two tailed T-test was performed to assess significance.

(D) Fusion peptide ELISA (average of n=2 technical replicates) was performed for a cohort of COVID naïve donors at various stages of vaccination. No significance was seen between groups in the development of FP specific antibodies. Limit of detection line is defined as the background binding of a negative control antibody to the FP for that experiment.

(E) Anti-Fusion Peptide ELISA (average of n=2 technical replicates) for longitudinal timepoints of donors who had a breakthrough infection between 2nd vaccine and bivalent. Pre-Breakthrough (Pre-BT) indicates the time point closest to (1-3 months) before breakthrough infection (BT) timepoint. A Kruskal Wallis one-way ANOVA was performed with Dunn's correction for multiple comparisons.

For A-E U/mL is defined as the reactivity seen by 1 μg/mL of 76E1 antibody[53]. Cutoffs were determined by binding of a negative control antibody (2A10).

STAR ★ METHODS

EXPERIMENTAL MODEL AND SUBJECT DETAILS

Human subjects

Use of human samples was approved by Partners Institutional Review Board (protocol 2020P002274). The current analysis is part of an ongoing study in which NH residents are consented directly or through their legally authorized representative if needed and serially sampled before and after each SARS-CoV-2 vaccine dose. This analysis includes data collected between September 29, 2021, and June 7, 2023. Residents who received SARS-CoV-2 mRNA vaccines [(BNT162b2 (Pfizer-BioNTech) or mRNA-1273 (Moderna)] were included, and those who received the Ad26.COV2.S (Janssen) vaccine were excluded. Participants received their first booster dose 8–9 months after the primary vaccination series, and their second booster 4 to 6 months after the first booster. We report results from blood samples obtained at time points prior to and following the two booster doses. All donor genders were self-reported.

Cell lines

HEK 293T cells (ATCC) were cultured in DMEM (Corning) containing 10% fetal bovine serum (VWR), and penicillin/streptomycin (Corning) at 37°C/5% CO_2. 293T-ACE2 cells were a gift from Michael Farzan (Scripps Florida) and Nir Hacohen (Broad Institute) and were cultured under the same conditions. Confirmation of ACE2 expression in 293T-ACE2 cells was done via flow cytometry. hDPP4-293T and hANPEP-293T were produced in-house and expression of hDPP4 and hANPEP was confirmed via flow cytometry.

METHOD DETAILS

To create variant spike expression plasmids, we performed multiple PCR fragment amplifications utilizing oligonucleotides containing each desired mutation (Integrated DNA Technology) and utilized overlapping fragment assembly to generate the full complement of mutations for each strain. PCR reactions were done with Platinum SuperFI II (Thermofisher) according to the manufacturer's protocol for reaction size and thermocycler protocol. Importantly, we generate these mutations in the context of our previously described (Garcia-Beltran *et al.* 2020[56]) codon-optimized SARS-CoV-2 spike expression plasmid harboring a deletion of the C-terminal 18 amino acids that was previously demonstrated to result in higher pseudovirus titers. Assembled fragments were inserted into NotI/XbaI digested pTwist-CMV-BetaGlobin-WPRE-Neo vector utilizing the In-Fusion HD Cloning Kit (Takara) according to the manufacturer's protocol. In-Fusion

reactions were transformed into Mix and Go DH5Alpha cells (Zymo Research) according to the manufacturer's protocol and colonies were grown overnight at 37˚C to generate plasmid DNA purified using a standard miniprep protocol (Qiagen). All resulting plasmid DNA utilized in the study was verified by whole-plasmid deep sequencing (Illumina or Primordium Labs) to confirm the presence of only the intended mutations and maxi-prepped (Macherey-Nagel) to ensure high quality, high concentrated DNA.

Construction of fusion and stem helix peptides

All peptides used in this manuscript were synthesized by GenScript with a C terminal cysteine for maleimide conjugation. The following sequences were used for the Fusion Peptide and Stem Helix: SKPSKRSFIEDLLNKVTLADAGC (FP), and DSFKEELDKYFKNHTSC (SH). Peptides were resuspended in the manufacturer recommended buffer, aliquoted into tubes, and stored at -20˚C when not in use.

SARS-CoV-2 pseudovirus neutralization assay

To compare the neutralizing activity of vaccine sera against coronaviruses, we produced lentiviral particles pseudotyped with different spike proteins as previously described (Garcia-Beltran *et al.* 2020[59]). Briefly, pseudoviruses were produced in 293T cells by PEI transfection of a lentiviral backbone encoding CMV-Luciferase-IRES-ZsGreen as well as lentiviral helper plasmids and each spike variant expression plasmid. Following collection and filtering, production was quantified by titering via flow cytometry on 293T-ACE2 cells. Neutralization assays and readout were performed on a Fluent Automated Workstation (Tecan) liquid handler using 384-well plates (Grenier). Three-fold serial dilutions ranging from 1:12 to 1:8,748 were performed for each serum sample before adding 125–250 infectious units of pseudovirus for 1 hr. Subsequently, 293T-ACE2 cells containing polybrene at 8 µg/mL were added to each well and incubated at 37°C/5% CO_2 for 48-60 hrs. Following transduction, cells were lysed using a luciferin-containing buffer (Siebring-van Olst *et al.* 2013[69]) and shaken for 5 min prior to quantitation of luciferase expression within 1 hr of buffer addition using a Spectramax L luminometer (Molecular Devices) or a Pherastar with Microplate Stacker (BMG Labtech). Percent neutralization was determined by subtracting background luminescence measured in cell control wells (cells only) from sample wells and dividing by virus control wells (virus and cells only). Data was analyzed using Graphpad Prism and pNT_{50} values were calculated by taking the inverse of the 50% inhibitory concentration value for all samples with a neutralization value of 80% or higher at the highest concentration of serum.

Titering

To determine the infectious units of pseudotyped lentiviral vectors, we plated 400,000 293T-ACE2 cells per well of a 12-well plate. 24 h later, three ten-fold serial dilutions of neat pseudovirus supernatant were made in 100 µL, which was then used to replace 100 µL of media on the plated cells. Cells were incubated for 48 h at 37°C/5% CO_2 to allow for expression of the ZsGreen reporter gene and harvested with Trypsin-EDTA (Corning). Cells were resuspended in PBS supplemented with 2% FBS (PBS+), and analyzed on a Stratedigm S1300Exi Flow Cytometer to determine the percentage of ZsGreen-expressing cells. Infectious units were calculated by determining the percentage of infected cells in wells exhibiting linear decreases in transduction and multiplying by the average number of cells per well determined at the initiation of the assay. At low MOI, each transduced ZsGreen cell was assumed to represent a single infectious unit.

hANPEP and hDPP4 293T Cell Line Production

To create cell lines that could be used in the high throughput neutralization assay we first cloned the known cellular receptors hDPP4 (MERS) and hANPEP (229E) into a lentiviral vector backbone from cDNA. Lentivirus was then produced using the same plasmids as the pseudovirus without the spike or fLuc-ZsGreen vectors. 293T cells were seeded at 400,000 cells/well one day before, media was removed and an equal quantity of lentivirus was added to cells. After 48 hours, cells were counted and diluted to 1 cell/well of 2 X 96 well plates. Single cell clones were then grown up for 2 weeks and assessed for surface expression of the indicated receptor by flow cytometry using the following stains CD26-PE-Cy7 (Biolegend 302713), or CD13-BV785 (Biolegend 301725). The highest expressing single clone was then grown up to make the cell line and frozen down in 90% FBS 10% DMSO for further uses.

Endpoint ELISA

Endpoint ELISAs were determined as follows: 96-well NUNC MaxiSorp ELISA plates (ThermoFisher) were coated with either purified S2P stabilized spike protein at 0.8 µg/mL or 1 µg/mL purified RBD (kindly provided by Aaron Schmidt, Jared Feldman, and Blake Hauser) or 2 µg/mL synthesized Stem-Helix or Fusion-Peptide (GenScript). Plates were washed with a wash buffer consisting of 50 mM Tris (pH 8.0) (Sigma), 140 mM NaCl (Sigma), and 0.05% Tween-20 (Sigma). Plates were incubated with a blocking buffer consisting of 1% BSA (Seracare), 50 mM Tris (pH 8.0), and 140 mM NaCl for 30 min at room temperature, and then washed. Serum samples were diluted 1:100 with a dilution buffer consisting of 1% BSA, 50 mM Tris (pH 8.0), 140 mM NaCl, and 0.05% Tween-20. Samples were added to corresponding wells and incubated for

1 hr at room temperature, followed by washing. Anti-human IgG-HRP (1:25,000) specific antibodies (Bethyl) were then used to detect bound serum antibodies and were diluted as indicated. These were added to each plate and incubated for 30 min at room temperature. After washing, detection was done with a TMB 2-Component Microwell Peroxidase Substrate Kit (VWR). Substrate B and Sample were mixed at a 1:1 ratio following manufacturer instructions and then added to each well and incubated for ~5 min before stopping with 3 M H2SO4. Buffer compositions, reagent concentrations and incubation times and temperatures were optimized in separate experiments for each analyte to maximize signal-to-noise ratio. Optical density (O.D.) was measured at 450 nm with subtraction of the O.D. at 570 nm as a reference wavelength on a SpectraMax ABS microplate reader. Antibody endpoint titer represents the maximum interpolated dilution that can still bind the antigen. The endpoint titers were evaluated at a top dilution of 100-fold with seven additional 3-fold serial dilutions. The wells incubated with no plasma incubation were used as controls, and cut-off values (used for interpolation) were defined as 2.1X the OD450 of the controls.

Quantitative ELISA

ELISAs were performed identically to endpoint ELISAs. A standard curve was generated using the following antibodies and the WT SARS-CoV-2 spike ectodomain (SinoBiologic) was used for coating at 0.8 µg/mL: RBD182 antibody as a control for Spike and SARS-CoV-2 RBD binding, S2P6 as a control for Stem Helix binding, and 76E1 as a control for Fusion Peptide binding. Anti-RBD and anti-spike antibody levels were calculated by interpolating onto the standard curve and correcting for sample dilution; one unit per mL (U/mL) was defined as the equivalent reactivity seen by 1 µg/mL of a SARS-CoV-2 RBD antibody we made in house (RBD182 was isolated from human donor PBMCs). Anti-SH and anti-FP antibodies were calculated similarly; one U/mL of SH antibody was defined as the equivalent reactivity seen by 1 µg/mL S2P6 while one U/mL of FP antibody was defined as the equivalent reactivity seen by 1 µg/mL 76E1.

Depletion Protocol RBD

Dynabeads (Thermofisher) were washed three times according to the manufacturer protocol and resuspended in PBS + 0.05% BSA. 5 µL of serum was added to molar equivalents of purified RBD (kindly provided by Aaron Schmidt, Jared Feldman, and Blake Hauser). Mock depleted sera was added to an equivalent volume of PBS + 0.05% BSA. Serum and RBD or serum and PBS + 0.05% BSA were incubated at room temperature for 1 hour. Beads were added to a magnet for 5

minutes, the supernatant was removed, and beads were resuspended in the RBD + Serum or Mock depletion mixture before incubating for 30 minutes at room temperature. Depletions were then placed on a magnetic strip for 5 minutes and supernatant was collected for downstream assays. RBD depletion was confirmed by an ELISA of mock and depleted samples for binding to the RBD.

Depletion Protocol Stem Helix and Fusion Peptide

Maleimide activated beads (Cube Biotech) were washed three times according to the manufacturer's protocols in coupling buffer. 3 mg of peptide was then added to the coupling buffer to a final volume of 1.5 mL in an Eppendorf tube. Beads were then resuspended in the coupling buffer with a peptide and incubated on a thermoshaker overnight at 4˚C or at 20˚C for 2 hours. Beads were then incubated on a magnetic strip for 2 minutes before being washed 3 more times in a coupling buffer and then once in 1 mL distilled water. Finally, conjugated beads were resuspended in 500 µL of storage buffer (Dissolve 2.1g of NaHCO3 in 150 mL water, adjust pH to 7.5 then add 1 mL sodium azide (5% w/v) and fill up to 250 mL with water) and stored at 4˚C for future use. Before depletion, beads were washed 3 times with PBS + 0.05% BSA and then resuspended in 5 µL Serum diluted in 45 µL PBS + 0.05% BSA before incubating at room temperature for 30 minutes. Beads were then incubated on a magnetic strip for 5 minutes before supernatant was removed for future analysis. Mock depletions were performed as above only with unconjugated beads. Depleted samples were confirmed by ELISA for both efficiency and selectivity of depletion.

QUANTIFICATION AND STATISTICAL ANALYSIS

Data and statistical analyses were performed using GraphPad Prism 10.2.2. Flow cytometry data was analyzed using FlowJo 10.10. One-way Anova and Mann Witney two-tailed T-tests were used in the indicated figures. Statistical significance was defined as $p < 0.05$.

REFERENCES

1. COVID - Coronavirus Statistics - Worldometer. https://www.worldometers.info/coronavirus/#google_vignette.
2. Greaney, A. J. *et al.* The SARS-CoV-2 Delta variant induces an antibody response largely focused on class 1 and 2 antibody epitopes. *PLoS Pathog.* **18**, e1010592 (2022).
3. Cox, M. *et al.* SARS-CoV-2 variant evasion of monoclonal antibodies based on in vitro studies. *Nat. Rev. Microbiol.* **21**, 112–124 (2023).
4. Cao, Y. *et al.* Omicron escapes the majority of existing SARS-CoV-2 neutralizing antibodies. *Nature* **602**, 657–663 (2022).
5. Starr, T. N., Greaney, A. J., Dingens, A. S. & Bloom, J. D. Complete map of SARS-CoV-2 RBD mutations that escape the monoclonal antibody LY-CoV555 and its cocktail with LY-CoV016. *Cell Rep. Med.* **2**, 100255 (2021).
6. Polack, F. P. *et al.* Safety and Efficacy of the BNT162b2 mRNA Covid-19 Vaccine. *New England Journal of Medicine* vol. 383 2603–2615 (2020).
7. Sadoff, J. *et al.* Safety and Efficacy of Single-Dose Ad26.COV2.S Vaccine against Covid-19. *New England Journal of Medicine* vol. 384 2187–2201 (2021).
8. Heath, P. T. *et al.* Safety and Efficacy of NVX-CoV2373 Covid-19 Vaccine. *New England Journal of Medicine* vol. 385 1172–1183 (2021).
9. Baden, L. R. *et al.* Efficacy and Safety of the mRNA-1273 SARS-CoV-2 Vaccine. *N. Engl. J. Med.* **384**, 403–416 (2021).
10. Hsieh, C.-L. *et al.* Structure-based design of prefusion-stabilized SARS-CoV-2 spikes. *Science* eabd0826 (2020) doi:10.1126/science.abd0826.
11. Garcia-Beltran, W. F. *et al.* Multiple SARS-CoV-2 variants escape neutralization by vaccine-induced humoral immunity. *Cell* **184**, 2372-2383.e9 (2021).
12. Plante, J. A. *et al.* Spike mutation D614G alters SARS-CoV-2 fitness. *Nature* **592**, 116–121 (2021).

13. Mlcochova, P. *et al.* SARS-CoV-2 B.1.617.2 Delta variant replication and immune evasion. *Nature* **599**, 114–119 (2021).
14. Lasrado, N. *et al.* Neutralization escape by SARS-CoV-2 Omicron subvariant BA.2.86. *Vaccine* **41**, 6904–6909 (2023).
15. Miller, J. *et al.* Substantial Neutralization Escape by SARS-CoV-2 Omicron Variants BQ.1.1 and XBB.1. *New England Journal of Medicine* vol. 388 662–664 (2023).
16. Jeworowski, L. M. *et al.* Humoral immune escape by current SARS-CoV-2 variants BA.2.86 and JN.1, December 2023. *Eurosurveillance* **29**, 2300740 (2024).
17. Roederer, A. L. *et al.* Ongoing evolution of SARS-CoV-2 drives escape from mRNA vaccine-induced humoral immunity. *Cell Rep. Med.* 101850 (2024) doi:10.1016/j.xcrm.2024.101850.
18. Bar-On, Y. M. *et al.* Protection of BNT162b2 Vaccine Booster against Covid-19 in Israel. *New England Journal of Medicine* vol. 385 1393–1400 (2021).
19. Link-Gelles, R. Effectiveness of Bivalent mRNA Vaccines in Preventing Symptomatic SARS-CoV-2 Infection — Increasing Community Access to Testing Program, United States, September–November 2022. *MMWR Morb. Mortal. Wkly. Rep.* **71**, (2022).
20. Tartof, S. Y. *et al.* BNT162b2 vaccine effectiveness against SARS-CoV-2 omicron BA.4 and BA.5. *Lancet Infect. Dis.* **22**, 1663–1665 (2022).
21. Uraki, R. *et al.* Antiviral and bivalent vaccine efficacy against an omicron XBB.1.5 isolate. *Lancet Infect. Dis.* **23**, 402–403 (2023).
22. Gayed, J. *et al.* Safety and Immunogenicity of the Monovalent Omicron XBB.1.5-Adapted BNT162b2 COVID-19 Vaccine in Individuals ≥12 Years Old: A Phase 2/3 Trial. *Vaccines* **12**, 118 (2024).
23. Hansen, C. H. *et al.* Short-term effectiveness of the XBB.1.5 updated COVID-19 vaccine against hospitalisation in Denmark: a national cohort study. *Lancet Infect. Dis.* **24**, e73–e74 (2024).

24. Chalkias, S. *et al.* Safety and Immunogenicity of XBB.1.5-Containing mRNA Vaccines. 2023.08.22.23293434 Preprint at https://doi.org/10.1101/2023.08.22.23293434 (2023).
25. Link-Gelles, R. Early Estimates of Updated 2023–2024 (Monovalent XBB.1.5) COVID-19 Vaccine Effectiveness Against Symptomatic SARS-CoV-2 Infection Attributable to Co-Circulating Omicron Variants Among Immunocompetent Adults — Increasing Community Access to Testing Program, United States, September 2023–January 2024. *MMWR Morb. Mortal. Wkly. Rep.* **73**, (2024).
26. Research, C. for B. E. and. Updated COVID-19 Vaccines for Use in the United States Beginning in Fall 2024. *FDA* (2024).
27. Xu, K. *et al.* Neutralization of SARS-CoV-2 KP.1, KP.1.1, KP.2 and KP.3 by human and murine sera. *Npj Vaccines* **9**, 1–6 (2024).
28. Kaku, Y. *et al.* Virological characteristics of the SARS-CoV-2 KP.2 variant. *Lancet Infect. Dis.* **0**, (2024).
29. GISAID Initiative. https://www.epicov.org/epi3/frontend#b40c.
30. Roederer, A. L. *et al.* Ongoing evolution of SARS-CoV-2 drives escape from mRNA vaccine-induced humoral immunity. 2024.03.05.24303815 Preprint at https://doi.org/10.1101/2024.03.05.24303815 (2024).
31. Planas, D. *et al.* Escape of SARS-CoV-2 Variants KP.1.1, LB.1, and KP3.3 From Approved Monoclonal Antibodies. *Pathog. Immun.* **10**, 1–11 (2024).
32. Vaccines and Related Biological Products Advisory Committee May 16, 2024 Meeting Announcement - 05/16/2024. *FDA* https://www.fda.gov/advisory-committees/advisory-committee-calendar/vaccines-and-related-biological-products-advisory-committee-may-16-2024-meeting-announcement (2024).
33. Walsh, J. A. & Maher, C. Economic Implications of Influenza and Influenza Vaccine. in *Influenza Vaccines for the Future* (eds. Rappuoli, R. & Del Giudice, G.) 425–440 (Springer, Basel, 2011). doi:10.1007/978-3-0346-0279-2_19.

34. Glennerster, R., Kelly, T., McMahon, C. T. & Snyder, C. M. Quantifying the Social Value of a Universal COVID-19 Vaccine and Incentivizing Its Development.
35. Starr, T. N. *et al.* SARS-CoV-2 RBD antibodies that maximize breadth and resistance to escape. *Nature* **597**, 97–102 (2021).
36. Wang, Y. *et al.* Identification of a highly conserved neutralizing epitope within the RBD region of diverse SARS-CoV-2 variants. *Nat. Commun.* **15**, 842 (2024).
37. Starr, T. N. *et al.* Shifting mutational constraints in the SARS-CoV-2 receptor-binding domain during viral evolution. *Science* **377**, 420–424 (2022).
38. Dacon, C. *et al.* Rare, convergent antibodies targeting the stem helix broadly neutralize diverse betacoronaviruses. *Cell Host Microbe* **31**, 97-111.e12 (2023).
39. Zhou, P. *et al.* Broadly neutralizing anti-S2 antibodies protect against all three human betacoronaviruses that cause deadly disease. *Immunity* **56**, 669-686.e7 (2023).
40. Pinto, D. *et al.* Broad betacoronavirus neutralization by a stem helix–specific human antibody. *Science* **373**, 1109–1116 (2021).
41. Wang, C. *et al.* A conserved immunogenic and vulnerable site on the coronavirus spike protein delineated by cross-reactive monoclonal antibodies. *Nat. Commun.* **12**, 1715 (2021).
42. Sun, X. *et al.* Neutralization mechanism of a human antibody with pan-coronavirus reactivity including SARS-CoV-2. *Nat. Microbiol.* **7**, 1063–1074 (2022).
43. Bianchini, F. *et al.* Human neutralizing antibodies to cold linear epitopes and subdomain 1 of the SARS-CoV-2 spike glycoprotein. *Sci. Immunol.* **8**, eade0958 (2023).
44. Dacon, C. *et al.* Broadly neutralizing antibodies target the coronavirus fusion peptide. *Science* **377**, 728–735 (2022).
45. Low, J. S. *et al.* ACE2-binding exposes the SARS-CoV-2 fusion peptide to broadly neutralizing coronavirus antibodies. *Science* **377**, 735–742 (2022).
46. Farrell, A. G. *et al.* Receptor binding domain (RBD) antibodies contribute more to SARS-CoV-2 neutralization when target cells express high levels of ACE2. *bioRxiv*

2022.08.29.505713 (2022) doi:10.1101/2022.08.29.505713.

47. Greaney, A. J. *et al.* Comprehensive mapping of mutations in the SARS-CoV-2 receptor-binding domain that affect recognition by polyclonal human plasma antibodies. *Cell Host Microbe* **29**, 463-476.e6 (2021).
48. Greaney, A. J. *et al.* Antibodies elicited by mRNA-1273 vaccination bind more broadly to the receptor binding domain than do those from SARS-CoV-2 infection. *Sci. Transl. Med.* **13**, eabi9915 (2021).
49. Li, Z. *et al.* The human coronavirus HCoV-229E S-protein structure and receptor binding. *eLife* **8**, e51230 (2019).
50. Breslin, J. J. *et al.* Human Coronavirus 229E: Receptor Binding Domain and Neutralization by Soluble Receptor at 37°C. *J. Virol.* **77**, 4435–4438 (2003).
51. Mou, H. *et al.* The Receptor Binding Domain of the New Middle East Respiratory Syndrome Coronavirus Maps to a 231-Residue Region in the Spike Protein That Efficiently Elicits Neutralizing Antibodies. *J. Virol.* **87**, 9379–9383 (2013).
52. Wang, N. *et al.* Structure of MERS-CoV spike receptor-binding domain complexed with human receptor DPP4. *Cell Res.* **23**, 986–993 (2013).
53. Sun, X. *et al.* Neutralization mechanism of a human antibody with pan-coronavirus reactivity including SARS-CoV-2. *Nat. Microbiol.* **7**, 1063–1074 (2022).
54. Ashkenazy, H. *et al.* ConSurf 2016: an improved methodology to estimate and visualize evolutionary conservation in macromolecules. *Nucleic Acids Res.* **44**, W344–W350 (2016).
55. Kleanthous, H. *et al.* Scientific rationale for developing potent RBD-based vaccines targeting COVID-19. *Npj Vaccines* **6**, 1–10 (2021).
56. Piccoli, L. *et al.* Mapping Neutralizing and Immunodominant Sites on the SARS-CoV-2 Spike Receptor-Binding Domain by Structure-Guided High-Resolution Serology. *Cell* **183**, 1024-1042.e21 (2020).
57. Liu, L. *et al.* Potent neutralizing antibodies against multiple epitopes on SARS-CoV-2 spike.

Nature **584**, 450–456 (2020).

58. Poh, C. M. *et al.* Two linear epitopes on the SARS-CoV-2 spike protein that elicit neutralising antibodies in COVID-19 patients. *Nat. Commun.* **11**, 2806 (2020).
59. Garcia-Beltran, W. F. *et al.* COVID-19-neutralizing antibodies predict disease severity and survival. *Cell* **184**, 476-488.e11 (2021).
60. Yang, Y. *et al.* Longitudinal analysis of antibody dynamics in COVID-19 convalescents reveals neutralizing responses up to 16 months after infection. *Nat. Microbiol.* **7**, 423–433 (2022).
61. Stewart-Jones, G. B. E. *et al.* Domain-based mRNA vaccines encoding spike protein N-terminal and receptor binding domains confer protection against SARS-CoV-2. *Sci. Transl. Med.* **15**, eadf4100 (2023).
62. Hsieh, C.-L. *et al.* Prefusion-stabilized SARS-CoV-2 S2-only antigen provides protection against SARS-CoV-2 challenge. *Nat. Commun.* **15**, 1553 (2024).
63. Halfmann, P. J. *et al.* Multivalent S2-based vaccines provide broad protection against SARS-CoV-2 variants of concern and pangolin coronaviruses. *EBioMedicine* **86**, 104341 (2022).
64. Kong, R. *et al.* Fusion peptide of HIV-1 as a site of vulnerability to neutralizing antibody. *Science* **352**, 828–833 (2016).
65. Wang, H. *et al.* Potent and broad HIV-1 neutralization in fusion peptide-primed SHIV-infected macaques. *Cell* **187**, 7214-7231.e23 (2024).
66. WHO chief declares end to COVID-19 as a global health emergency | UN News. https://news.un.org/en/story/2023/05/1136367 (2023).
67. Statement on the fifteenth meeting of the IHR (2005) Emergency Committee on the COVID-19 pandemic. https://www.who.int/news/item/05-05-2023-statement-on-the-fifteenth-meeting-of-the-international-health-regulations-(2005)-emergency-committee-regarding-the-coronavirus-disease-(covid-19)-pandemic.

68. Roederer, A. L. *et al.* Ongoing evolution of SARS-CoV-2 drives escape from mRNA vaccine-induced humoral immunity. *Cell Rep. Med.* **5**, 101850 (2024).

69. Siebring-van Olst, E. *et al.* Affordable luciferase reporter assay for cell-based high-throughput screening. *J. Biomol. Screen.* **18**, 453–461 (2013).

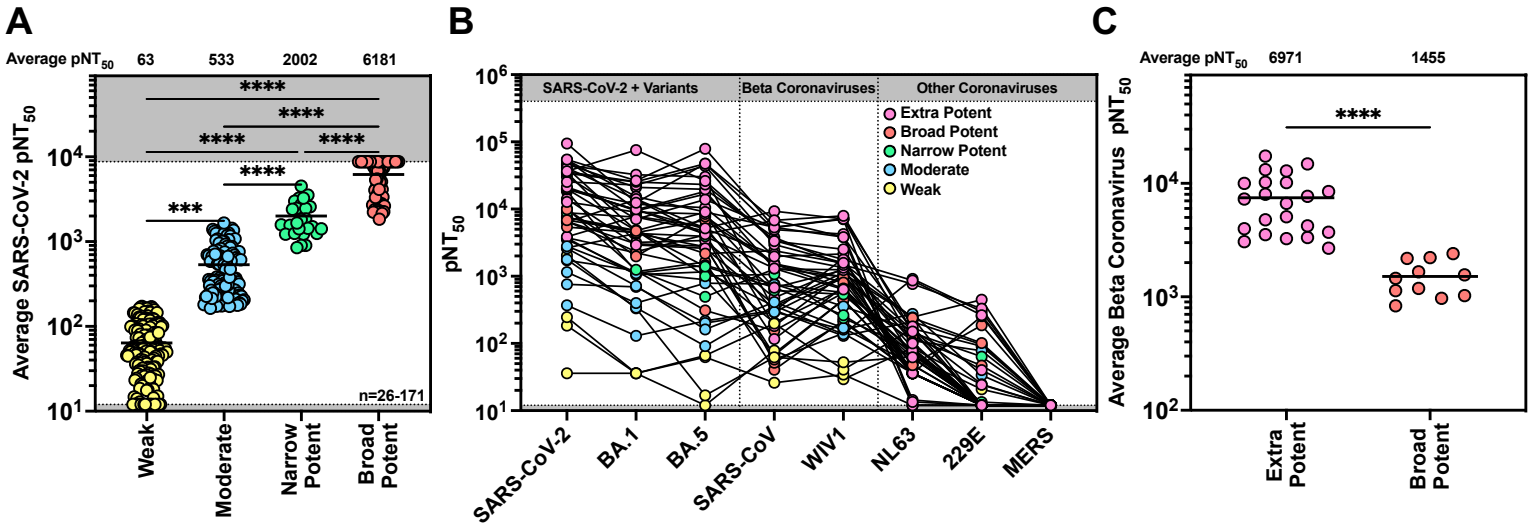

Figure 1: Broad neutralizers have extensive breadth across related Betacoronaviruses.

(A) Cohort of 399 donor samples divided into 4 groups by average neutralization potency (average of n=2 technical replicates) across SARS-CoV-2 WT and the BA.1 and BA.5 variants. Groups were compared using a One-Way ANOVA with Holm-Šídák correction for multiple comparisons using statistical hypothesis testing **** = P<0.0001.

(B) 14 of the broadest neutralizers were subject to our high throughput neutralization assay against SARS-CoV-2, variants, SARS-like viruses, and other distantly related coronaviruses with a much higher threshold for neutralizing activity (average of n=2 technical replicates) . These donors were further subdivided into Super Potent and Broad Potent based on average neutralizing activity.

(C) Neutralizing activity (average of n=2 technical replicates) of donors averaged across Beta Coronaviruses (excluding MERS). Groups were compared using a two tailed Mann-Whitney T test with P = 0.0007.

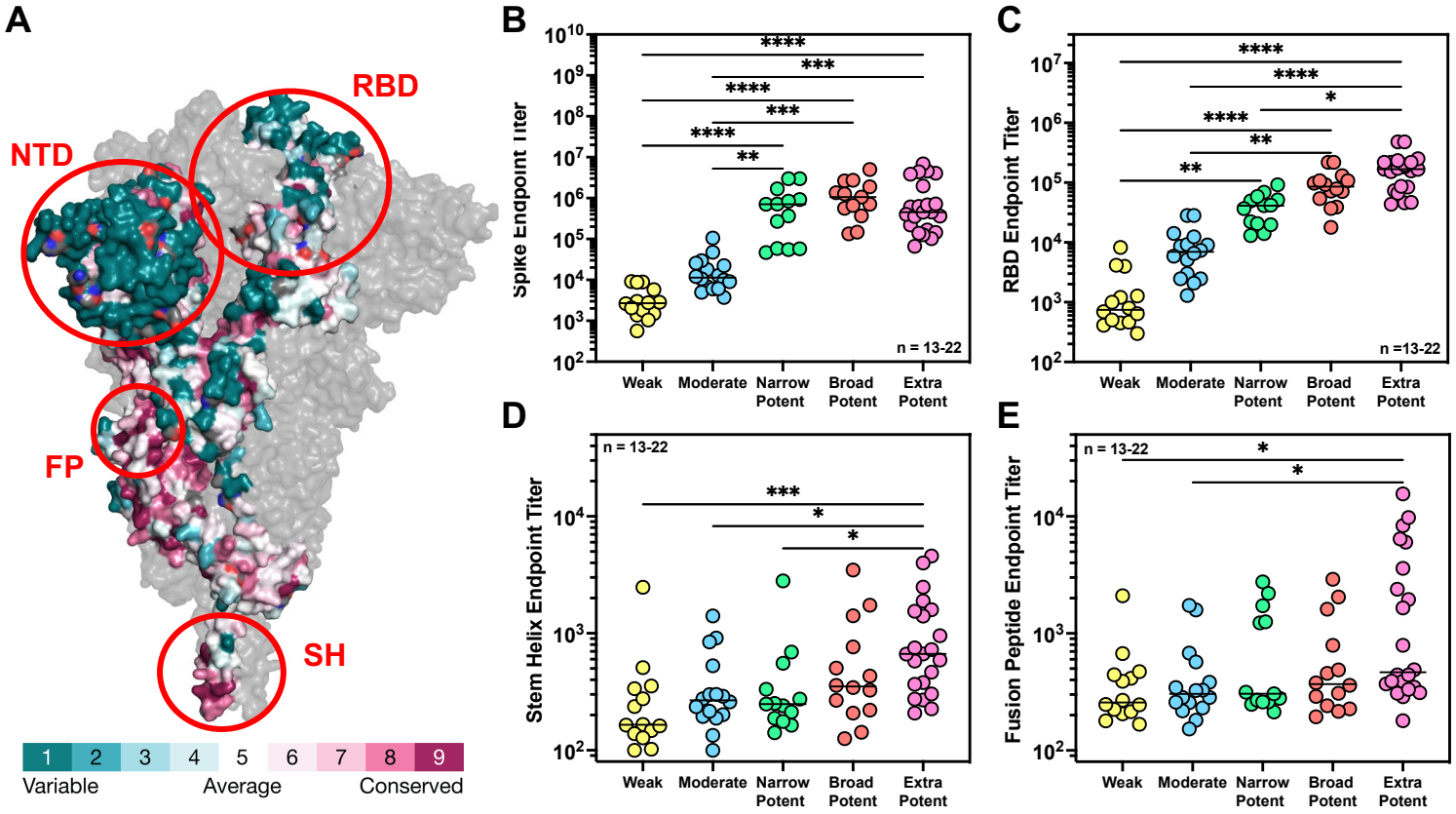

Figure 2: Extra potent sera have the highest levels of RBD, SH and FP Antibodies.
(A) Conservation of the amino acids within the spike protein generated using consurf[50] from (PDB 6XR8[59] https://doi.org/10.2210/pdb6xr8/pdb). The sequences fed into the algorithm include 59 coronavirus spike sequences representing all four clades. RBD = Receptor Binding Domain, NTD = N-Terminal Domain, FP = Fusion Peptide, SH = Stem Helix.
(B-E) Results from ELISA assessing the antibody endpoint titers of plasma from 22 extra potent, 13 Broad/Potent, 13 Narrow/Potent, 16 Moderate and 14 Weak donors. Antibody endpoint titers (average of n=2 technical replicates) were assessed against an S2P Stabilized spike (B), Receptor Binding Domain (C), Stem Helix Peptide (D), or Fusion Peptide (E). Antibody endpoint titer represents the maximum interpolated dilution that can still bind the antigen. The endpoint titers were evaluated at a top dilution of 100-fold with seven additional 3-fold serial dilutions. The wells incubated with no plasma incubation were used as controls, and cut-off values (used for interpolation) were defined as 2.1X the OD450 of the controls. Representative data from two independent experiments is shown. Groups were compared using a One Way ANOVA with Kruskal Wallis Test and Dunn's multiple comparisons test. (* = P<0.0332, ** = P<0.0021, ***= P<0.0002, ****= P<0.0001).

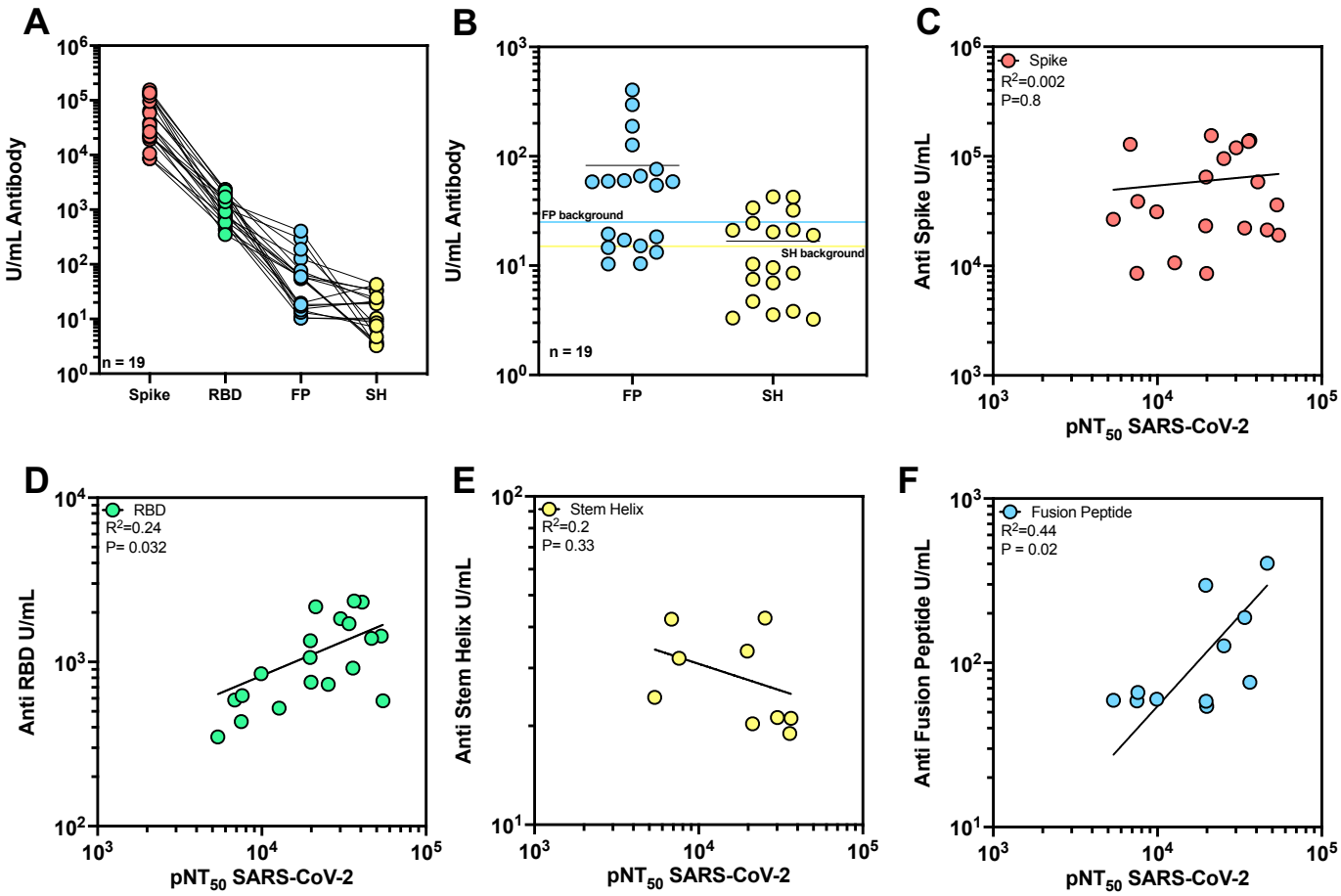

Figure 3: RBD and fusion peptide specific antibody titers correlate with neutralizing activity.
(A) U/mL of antigen specific antibody was assessed for a cohort of broad and potent neutralizers (average of n=2 technical replicates). All U/mL were calculated using an antigen specific ELISA and were defined as the equivalent reactivity to 1 µg/mL binding of the following antibodies: RBD182 (Spike, RBD), 76E1 (FP), S2P6 (SH).
(B) All donors from A were tested for binding to the Stem Helix or Fusion Peptide along with a negative control antibody (2A10) at the same concentration as the serum dilution to determine cutoffs to define background serum binding.
(C-F) Log-log regression analyses were performed on neutralization versus anti-Spike IgG (C), anti-RBD IgG (D), anti-SH IgG (E), and anti-FP IgG (F). Pearson correlations were performed and R^2 and p values are indicated.

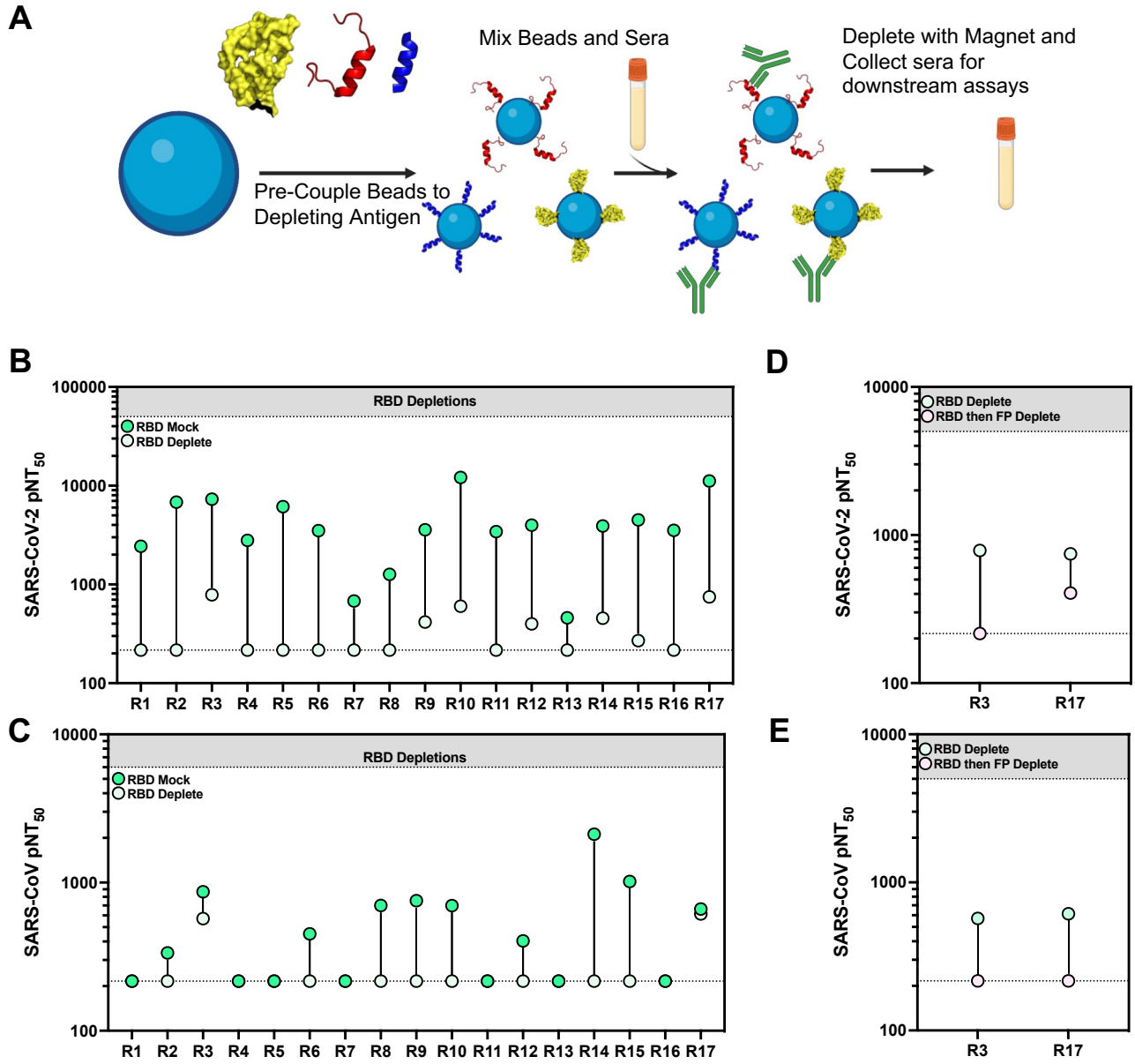

Figure 4: Fusion peptide antibodies contribute to neutralization breadth.

(A) Schematic detailing our antigen depletion protocol. Briefly, his-tag or maleimide binding magnetic beads are pre-coupled to the antigen/peptide and mixed with serum. After an incubation the magnetic beads are pulled away using a magnet and serum is collected for downstream assays. Mock depletion is done by mixing serum and beads with no antigen (Created in BioRender).

(B-C) Serum samples with high neutralizing activity were subject to RBD based depletion using his-tagged beads or mock depletion using beads with no RBD bound. Mock and depleted serum was tested for neutralizing activity (average of n=2 technical replicates) against SARS-CoV-2 (C) and SARS-CoV (D).

(D-E) Serum samples with remaining neutralizing activity against both SARS-CoV-2 and SARS-CoV from (B-C) were subject to further depletion with the fusion peptide and tested for remaining neutralizing activity (average of n=2 technical replicates) to SARS-CoV-2 (D) and SARS-CoV (E) after double depletion.

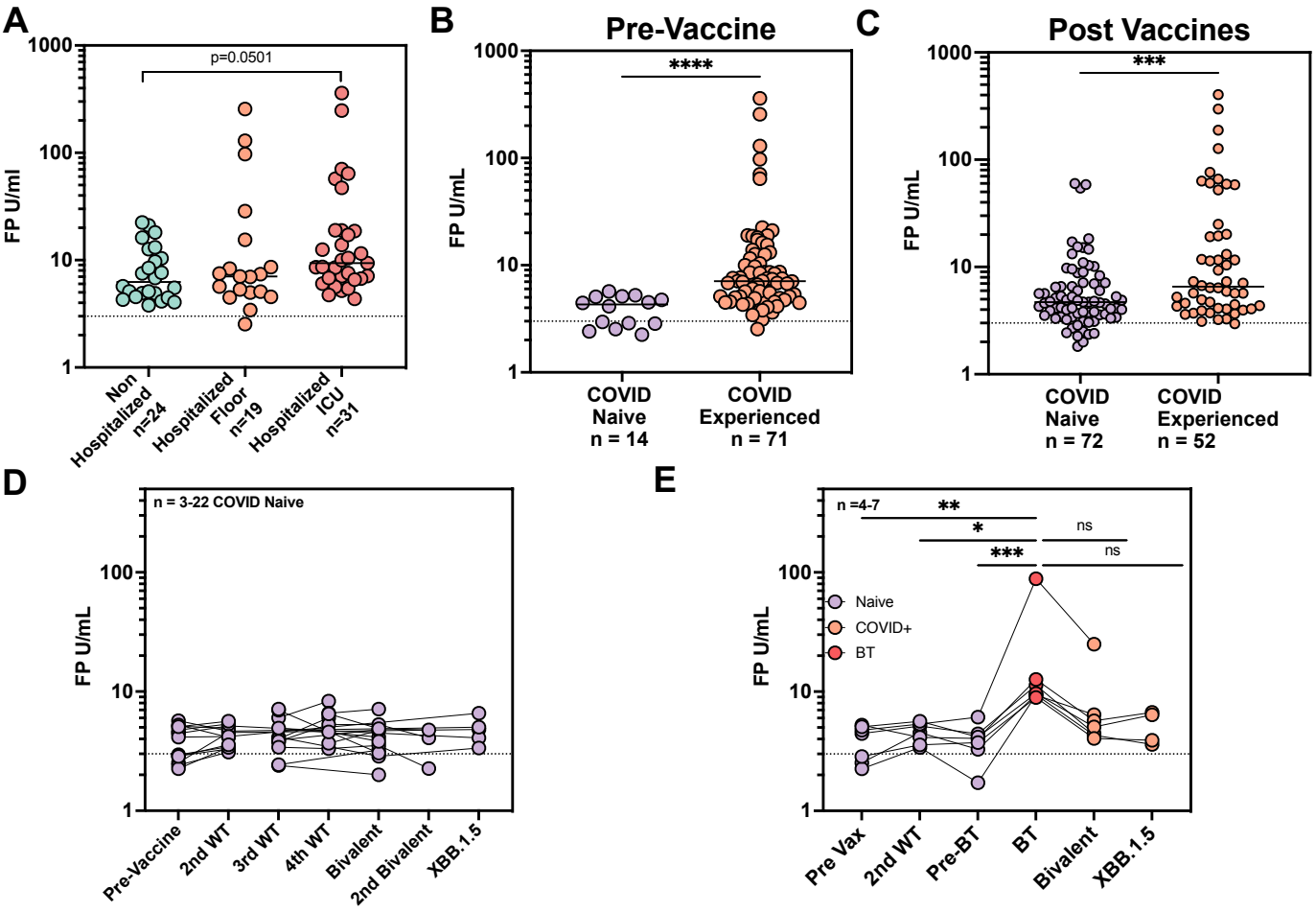

Figure 5: Fusion peptide antibodies develop in response to natural infection.

(A) Anti-Fusion Peptide ELISA for a cohort of COVID+ pre-vaccination timepoints split into non-hospitalized and severity of hospitalization (average of n=2 technical replicates). Limit of detection line is defined as the background binding of a negative control antibody to the FP for that experiment. A Kruskal Wallis one-way ANOVA was performed with Dunn's correction for multiple comparisons.

(B) Anti-Fusion Peptide ELISA (average of n=2 technical replicates) for pre-vaccination serum samples for donors who were naïve or who had been infected with COVID. A Mann Whitney Two tailed T-test was performed to assess significance.

(C) Anti-Fusion Peptide ELISA (average of n=2 technical replicates) for post-vaccination serum samples for donors who were naïve after 2-6 vaccines or who were COVID+ at the timepoint and had received between 2-6 vaccines. A Mann Whitney Two tailed T-test was performed to assess significance.

(D) Fusion peptide ELISA (average of n=2 technical replicates) was performed for a cohort of COVID naïve donors at various stages of vaccination. No significance was seen between groups in the development of FP specific antibodies. Limit of detection line is defined as the background binding of a negative control antibody to the FP for that experiment.

(E) Anti-Fusion Peptide ELISA (average of n=2 technical replicates) for longitudinal timepoints of donors who had a breakthrough infection between 2nd vaccine and bivalent. Pre-Breakthrough (Pre-BT) indicates the time point closest to breakthrough infection (BT) timepoint. A Kruskal Wallis one-way ANOVA was performed with Dunn's correction for multiple comparisons.

For A-E U/mL is defined as the reactivity seen by 1 µg/mL of 76E1 antibody[53]. Cutoffs were determined by binding of a negative control antibody (2A10).

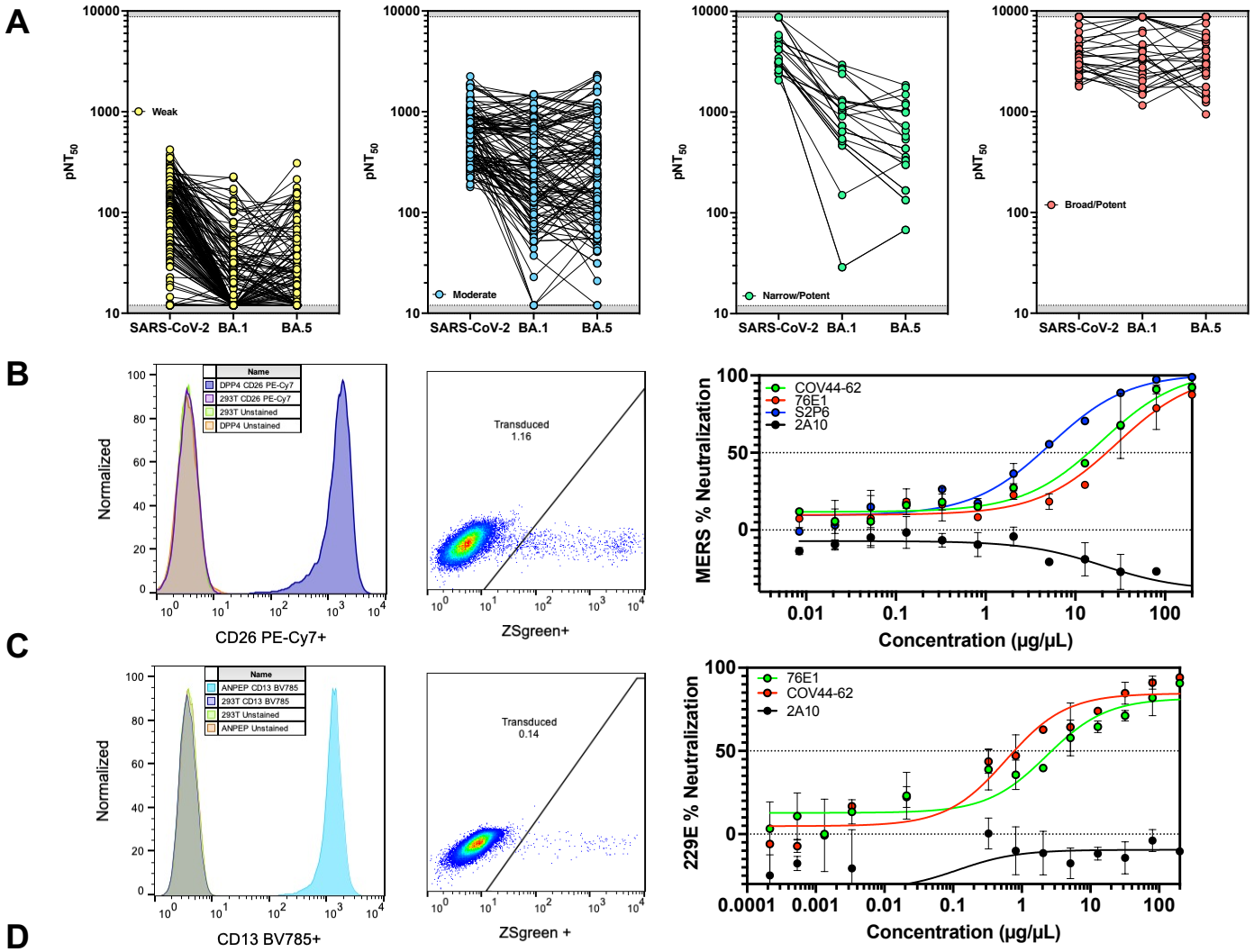

Antibody	Virus	IC_{50} Literature	IC_{50} Calculated
76E1	MERS	3.825 µg/mL	28.8 µg/mL
S2P6	MERS	17 µg/mL	5.23 µg/mL
COV44-62	MERS	25 µg/mL	19.77 mg/mL
COV44-62	229E	2.11 µg/mL	0.594 µg/mL
76E1	229E	1.16 µg/mL	2.31 µg/mL

Figure S1 (related to **Fig. 1**)**: Individual neutralization values for donor cohort and development and validation of MERS and 229E neutralization assays.**

(A) Neutralization Assay (average of n=2 technical replicates) against SARS-CoV-2 and BA.1, BA.5 Variants for a cohort of 399 donor samples.

(B-C) Adaptation of our high throughput neutralization assay to evaluate MERS (B) and 229E (C) neutralization. We transduced 293T cells to express either hDPP4 (C) or hANPEP (B) and confirmed cell-surface expression by flow cytometry (Left). These cell lines were tested for transduction by MERS (B) or 229E (C) pseudoviruses, respectively (Middle). Finally, we performed neutralization assays with known neutralizing antibodies COV44-62, 76E1, and S2P6 and 2A10 as a negative control to evaluate these cell lines and pseudoviruses (Right). Data represented as mean +/- SD.

(D) Table comparing the IC_{50} values for antibodies in the literature relative to IC_{50} values we calculated.

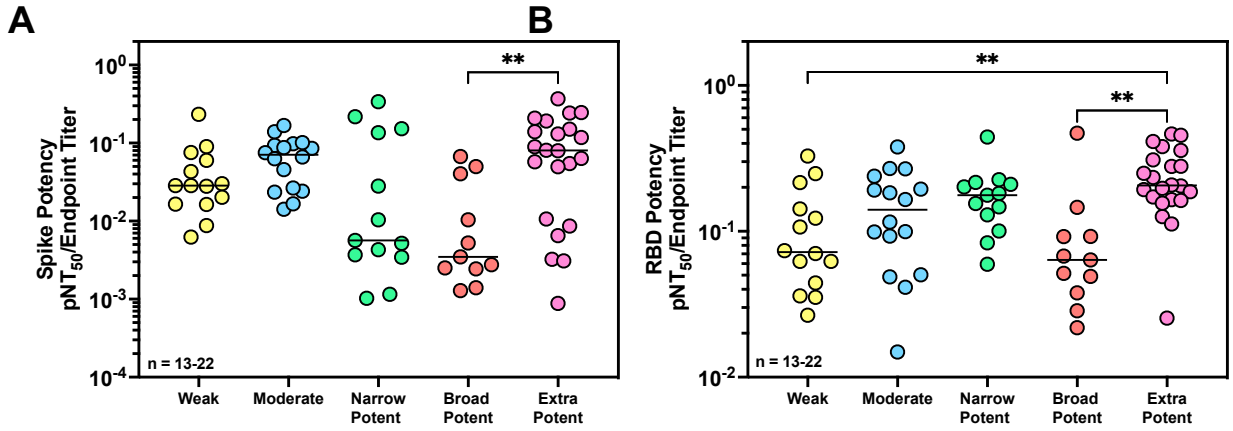

Figure S2 (related to **Fig. 2**)**: Extra potent donors have potent RBD specific antibodies.**
(A-B) Neutralization potency index (pNT_{50} WT value / Endpoint titer for average of n=2 technical replicates) for Spike (A), and RBD (B). Groups were compared using a One Way ANOVA with Kruskal Wallis Test and Dunn's multiple comparisons test. (* = P<0.0332, ** = P<0.0021, ***= P<0.0002, ****= P<0.0001).

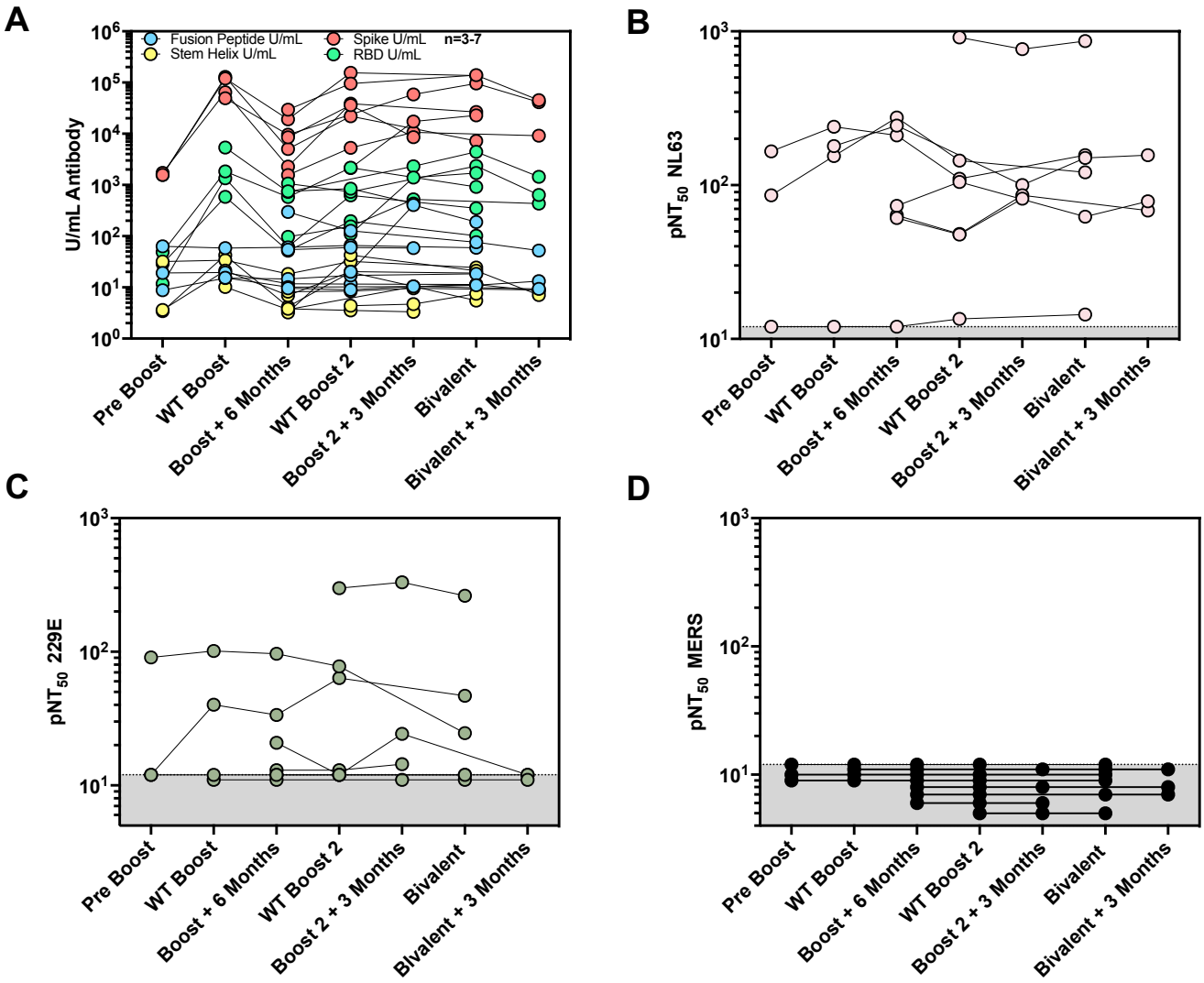

Figure S3 (related to **Fig. 3**)**: Repeated vaccination does not correlate with antigen specific antibodies, nor does it increase neutralization against alpha coronaviruses or MERS.**
(A) ELISA (average of n=2 technical replicates) results for anti-SARS-CoV-2 Spike, anti-RBD, anti-Stem Helix, and anti-Fusion Peptide directed antibodies. One U/mL is defined as the equivalent reactivity seen by 1 µg/mL RBDCOV182 antibody or 1 µg/mL S2P6 for SH or 1 µg/mL 76E1 for FP. Each line corresponds to a single donor over time.
(B-D). Neutralizing titer (average of n=2 technical replicates) against NL63 (B), 229E (C), or MERS (D) was assessed for longitudinal timepoints. Each line corresponds to a single donor over time.

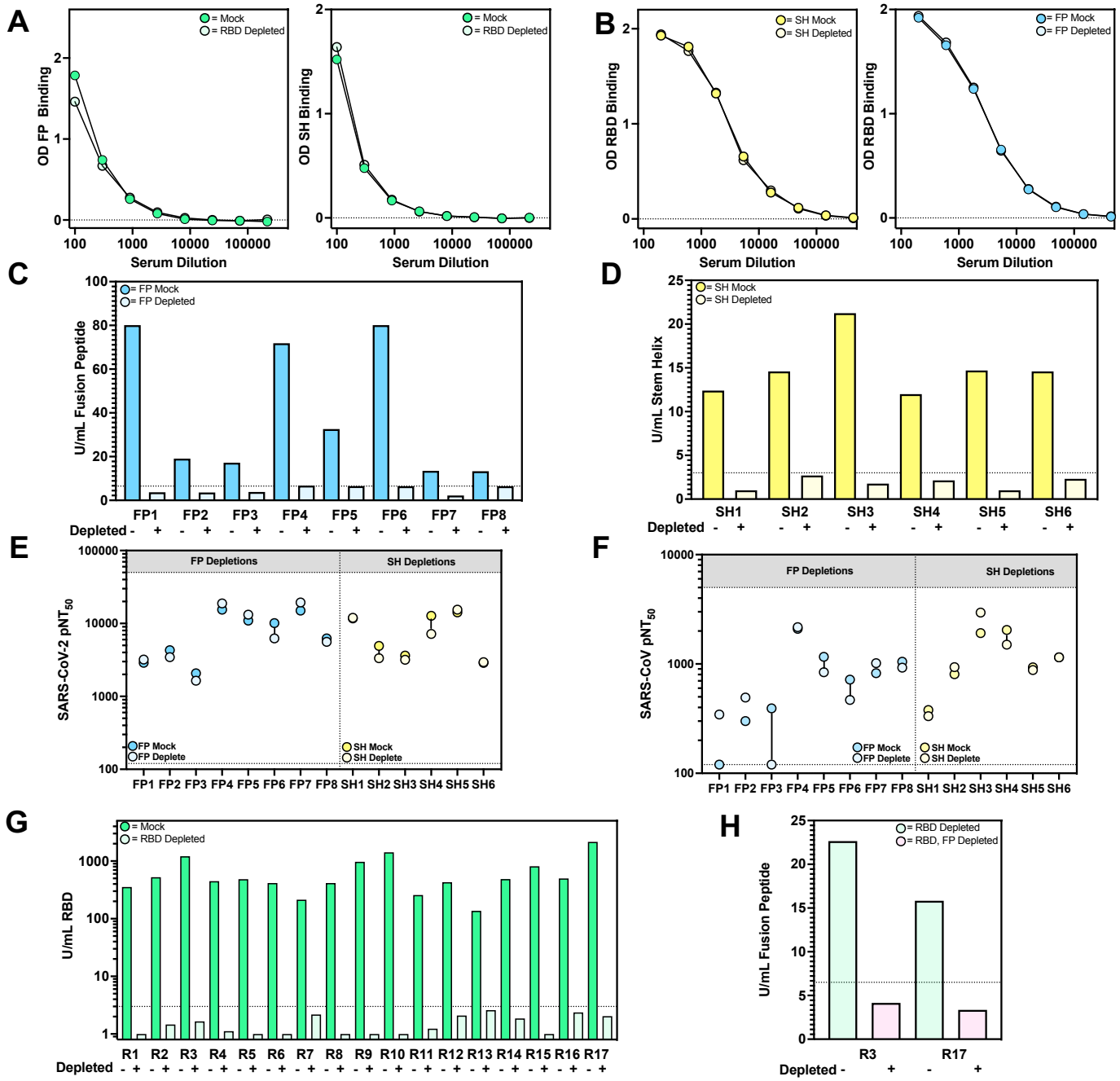

Figure S4 (related to **Fig, 4**): **Antigen depletions effectively remove antigen specific antibodies.**

(A) Selectivity of RBD depletion. Serum samples were subject to Mock or RBD depletion and then tested by ELISA (average of n=2 technical replicates) for binding to either the Fusion Peptide (left) or Stem Helix (right). Two representative samples are shown for each depletion for samples that had strong binding to either the FP or the SH.

(B) Selectivity of Fusion Peptide or Stem Helix Depletion. Serum samples were subject to depletion against either the FP (left) or the SH (right) and then tested for binding to RBD by an ELISA (average of n=2 technical duplicates). Two representative samples are shown for each depletion.

(C-D) Depletion ELISA detailing the effect of FP (C), SH (D) depletion on 6-8 broadly neutralizing donor timepoints. Donors with high FP or SH binding were chosen for depletion with those antigens U/mL is calculated with 1 U/mL defined as the equivalent reactivity seen by 1 µg/mL, 76E1[37] for FP and S2P6[35] for SH. Cutoffs were defined by a negative control antibody (2A10).

(E-F) Serum samples were subject to either fusion peptide or stem helix depletion to remove peptide specific antibodies and then tested for neutralizing activity (average of n=2 technical replicates) to either SARS-CoV-2 (E) or SARS-CoV (F). Mock samples were combined with beads only for mock depletion.

(G) Depletion ELISA (average of n=2 technical replicates) detailing the effect of RBD (F) depletion on 18 broadly neutralizing donor timepoints. Timepoints with high FP or SH binding were chosen for depletion with those antigens U/mL is calculated with 1 U/mL defined as the equivalent reactivity seen by 1 µg/mL RBDCOV182(isolated in house) antibody for RBD. Cutoffs were defined by a negative control antibody (2A10).

(H) RBD Depleted donors with remaining neutralizing activity were subject to fusion peptide depletion and an ELISA (average of n=2 technical replicates) was done to confirmed depletion. Cutoffs were defined by a negative control antibody (2A10).

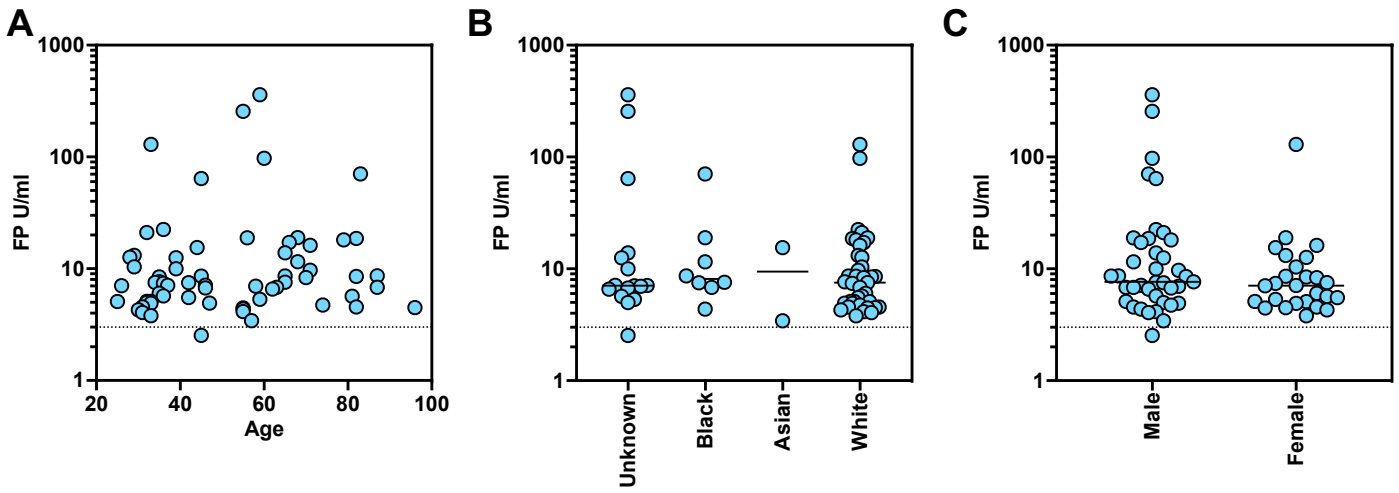

Figure S5 (related to **Fig. 5**): **Age, race, and biological sex did not correlate with FP antibody development.**
(A-C) Fusion peptide U/mL ELISA (average of n=2 technical replicates) for COVID+ donors separated by age (A), race (B), biological sex (C). Age, race and biological sex were not correlated with FP-specific antibodies.
For A-C U/mL is defined as the reactivity seen by 1 μg/mL of 76E1[37] antibody. Cutoffs were determined by binding of a negative control antibody (2A10).

Donor	Age	Biological Sex	Vaccination Status	Infection History
1	81-85	Male	4xWT, 1xBivalent	Infection Prior to 1st Vax
2	66-70	Female	4xWT, 1xBivalent	Naive
3	55-60	Male	4xWT, 1xBivalent	Infection Prior to 1st Vax
4	61-65	Male	4xWT, 1xBivalent	Naive
5	61-65	Female	4xWT, 1xBivalent	Infection After 4th Vax
6	66-70	Female	4xWT, 1xBivalent	Infection Prior to 1st Vax
7	86-90	Female	4xWT, 1xBivalent	Naive
8	76-70	Male	4xWT, 1xBivalent	Infection Prior to 1st Vax Infection after 4th Vax

Table S1 (related to **Fig 3,4**)**: Demographics of longitudinal donor cohort.**

Table describing individual timepoints from 8 of the broadest neutralizing donors spanning 3-5 timepoints including those 2-4 weeks after vaccination as well as timepoints that were distant (Post) from the nearest vaccination (3-6 months post) from a cohort of Nursing Home Samples.

Cohort	Statistics
Total (n)	255
Demographics All Cohorts	
Age (y) (median, range)	69 (25-96)
Biological Sex (% Female)	93/255 (36%)
COVID+ Pre-Vaccination Total (n)	74
Age (y) (median, range)	63 (25-96)
Biological Sex (% Female)	27/74 (36.4%)
Biological Sex (% Female)	6/20 (30%)
COVID Naïve Pre-Vaccine Total (n)	14
Age (y) (median, range)	70 (60-88)
Biological Sex (% Female)	3/14 (21%)
COVID Experienced Pre-Vaccine Total (n)	71
Age (y) (median, range)	55 (25-96)
Biological Sex (% Female)	29/71 (41%)
COVID Naïve Post-Vaccine (5C) Total (n)	72
Age (y) (median, range)	73 (49-89)
Biological Sex (% Female)	35/72 (49%)
COVID Experienced Post-Vaccine (5C) Total (n)	52
Age (y) (median, range)	70 (37-88)
Biological Sex (% Female)	13/52 (25%)
COVID Naïve Longitudinal (5D) Total (n)	30
Age (y) (median, range)	73 (49-88)
Biological Sex (% Female)	10/30 (33%)
Longitudinal BT Cohort (5E) Total (n)	7
Age (y) (median, range)	73 (65-88)
Biological Sex (% Female)	2/7 (29%)

Table S2 (related to **Fig 5**)**: Cohort Descriptions for Figure 5**
Descriptions of the various cohorts for Figure 5 and Supplemental Figure 5 with age and sex noted.